

# Search for the Decay $K_L^0 \rightarrow \pi^0 \nu \bar{\nu}$

J. K. Ahn,<sup>1</sup> Y. Akune,<sup>2</sup> V. Baranov,<sup>3</sup> K. F. Chen,<sup>4</sup> J. Comfort,<sup>5</sup> M. Doroshenko,<sup>6,\*</sup> Y. Fujioka,<sup>2</sup> Y.B. Hsiung,<sup>4</sup> T. Inagaki,<sup>6,7</sup> S. Ishibashi,<sup>2</sup> N. Ishihara,<sup>7</sup> H. Ishii,<sup>8</sup> E. Iwai,<sup>8</sup> T. Iwata,<sup>9</sup> I. Kato,<sup>9</sup> S. Kobayashi,<sup>2</sup> T. K. Komatsubara,<sup>7</sup> A. S. Kurilin,<sup>3</sup> E. Kuzmin,<sup>3</sup> A. Lednev,<sup>10,11</sup> H. S. Lee,<sup>1</sup> S. Y. Lee,<sup>1</sup> G. Y. Lim,<sup>7</sup> J. Ma,<sup>11</sup> T. Matsumura,<sup>12</sup> A. Moisseenko,<sup>3</sup> H. Morii,<sup>13</sup> T. Morimoto,<sup>7</sup> T. Nakano,<sup>14</sup> H. Nanjo,<sup>13</sup> J. Nix,<sup>11</sup> T. Nomura,<sup>13</sup> M. Nomachi,<sup>8</sup> H. Okuno,<sup>7</sup> K. Omata,<sup>7</sup> G. N. Perdue,<sup>11</sup> S. Podolsky,<sup>3,†</sup> K. Sakashita,<sup>8,‡</sup> T. Sasaki,<sup>9</sup> N. Sasao,<sup>13</sup> H. Sato,<sup>9</sup> T. Sato,<sup>7</sup> M. Sekimoto,<sup>7</sup> T. Shinkawa,<sup>12</sup> Y. Sugaya,<sup>8</sup> A. Sugiyama,<sup>2</sup> T. Sumida,<sup>13</sup> S. Suzuki,<sup>2</sup> Y. Tajima,<sup>9</sup> S. Takita,<sup>9</sup> Z. Tsamalaidze,<sup>3</sup> T. Tsukamoto,<sup>2,§</sup> Y. C. Tung,<sup>4</sup> Y. Wah,<sup>11</sup> H. Watanabe,<sup>11,‡</sup> M. L. Wu,<sup>4</sup> M. Yamaga,<sup>7,¶</sup> T. Yamanaka,<sup>8</sup> H. Y. Yoshida,<sup>9</sup> and Y. Yoshimura<sup>7</sup>

(E391a Collaboration)

<sup>1</sup>Department of Physics, Pusan National University, Busan, 609-735 Republic of Korea

<sup>2</sup>Department of Physics, Saga University, Saga, 840-8502 Japan

<sup>3</sup>Laboratory of Nuclear Problems, Joint Institute for Nuclear Research, Dubna, Moscow Region, 141980 Russia

<sup>4</sup>Department of Physics, National Taiwan University, Taipei, Taiwan 10617 Republic of China

<sup>5</sup>Department of Physics and Astronomy, Arizona State University, Tempe, Arizona, USA

<sup>6</sup>Department of Particle and Nuclear Research, The Graduate University for Advanced Science (SOKENDAI), Tsukuba, Ibaraki, 305-0801 Japan

<sup>7</sup>Institute of Particle and Nuclear Studies, High Energy Accelerator Research Organization (KEK), Tsukuba, Ibaraki, 305-0801 Japan

<sup>8</sup>Department of Physics, Osaka University, Toyonaka, Osaka, 560-0043 Japan

<sup>9</sup>Department of Physics, Yamagata University, Yamagata, 990-8560 Japan

<sup>10</sup>Institute for High Energy Physics, Protvino, Moscow region, 142281 Russia

<sup>11</sup>Enrico Fermi Institute, University of Chicago, Chicago, Illinois 60637, USA

<sup>12</sup>Department of Applied Physics, National Defense Academy, Yokosuka, Kanagawa, 239-8686 Japan

<sup>13</sup>Department of Physics, Kyoto University, Kyoto, 606-8502 Japan

<sup>14</sup>Research Center of Nuclear Physics, Osaka University, Ibaraki, Osaka, 567-0047 Japan

(Dated: April 24 2008)

We performed a search for the  $K_L^0 \rightarrow \pi^0 \nu \bar{\nu}$  decay at the KEK 12-GeV proton synchrotron. No candidate events were observed. An upper limit on the branching ratio for the decay was set to be  $6.7 \times 10^{-8}$  at the 90% confidence level.

PACS numbers: 13.20.Eb, 11.30.Er, 12.15.Hh

The decay  $K_L^0 \rightarrow \pi^0 \nu \bar{\nu}$  occurs via loop diagrams that change the quark flavor from strange to down [1]. It violates CP symmetry directly, and the amplitude is proportional to the imaginary part of the Cabbibo-Kobayashi-Maskawa matrix elements in the standard model (SM). Since the theoretical uncertainty in the branching ratio is small and controlled, it provides a good testing ground of the SM and beyond [2]. The branching ratio  $Br(K_L^0 \rightarrow \pi^0 \nu \bar{\nu})$  is predicted to be  $(2.49 \pm 0.39) \times 10^{-11}$  [3]. The current experimental limit is  $2.1 \times 10^{-7}$  at the 90% confidence level by our previous search [4].

KEK E391a is the first experiment dedicated to the  $K_L^0 \rightarrow \pi^0 \nu \bar{\nu}$  decay. Neutral kaons were produced by 12 GeV protons incident on a 0.8-cm-diameter and 6-cm-long platinum target. The proton intensity was typically  $2 \times 10^{12}$  per spill coming every 4 sec. The neutral beam [5], with a solid angle of  $12.6 \mu\text{str}$ , was defined by a series of six sets of collimators and a pair of sweeping magnets aligned at a production angle of 4 degrees. A 7-cm-thick lead block and a 30-cm-thick beryllium block were placed between the first and second collimators to reduce beam photons and neutrons. The  $K_L^0$  momentum

peaked around 2 GeV/c at the entrance of the detector, 11 m downstream from the target.

Figure 1 shows the cross-sectional view of the E391a detector.  $K_L^0$ 's entered from the left side, and the detector components were cylindrically assembled along the beam axis. Most of them were installed inside the vacuum tank to minimize interactions of the particles before detection. The electromagnetic calorimeter, labeled "CsI", measured the energy and position of the two photons from  $\pi^0$ . It consisted of 496 blocks of  $7 \times 7 \times 30 \text{ cm}^3$

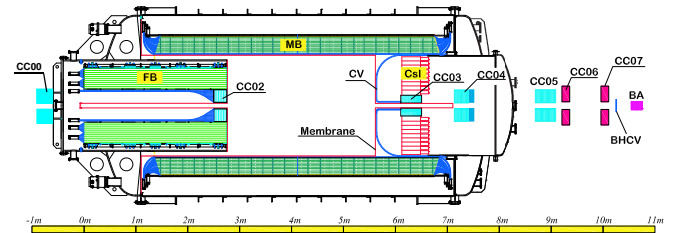


FIG. 1: (color online) Schematic cross-sectional view of the E391a detector. "0m" in the scale corresponds to the entrance of the detector.

undoped CsI crystal and 80 specially shaped CsI blocks used in the peripheral region, covering a  $190\text{ cm-}\phi$  circular area. To allow beam particles to pass through, the calorimeter had a  $12 \times 12\text{ cm}^2$  hole at the center. The main barrel (MB) and front barrel (FB) counters consisted of alternating layers of lead and scintillator sheets with total thicknesses of  $13.5 X_0$  and  $17.5 X_0$ , respectively, and surrounded the decay region. To identify charged particles entering the calorimeter, scintillation counters (CV) hermetically covered the front of the calorimeter. It consisted of a plastic scintillator hodoscope that were placed  $50\text{ cm}$  upstream of the calorimeter and four  $6\text{-mm-thick}$  scintillator plates that were located parallel to the beam axis between the hodoscope and the calorimeter. Multiple collar-shaped photon counters (CC00, CC02–07) were placed along the beam axis to detect particles escaping in the beam direction. CC02 was a shashlik type lead-scintillator sandwich counter, and was located at the upstream end of the  $K_L^0$  decay region. CC03 filled the volume between the beam hole and the innermost layers of the CsI blocks in the calorimeter. The vacuum region was separated by a thin multi-layer film (“membrane”) into the beam and detector regions. This kept the decay region at  $1 \times 10^{-5}\text{ Pa}$  despite some outgassing from the detector. Further descriptions of the E391a detector are given in [4, 6].

The E391a experiment started taking data in February 2004. In the first period, whose partial analysis was reported in [4], the membrane drooped into the neutral beam near the calorimeter and caused many neutron-induced backgrounds. After fixing this problem, we resumed the physics run in 2005. In this analysis, we used the data in the second period from February to April 2005. Data were taken with a hardware trigger requiring two or more shower clusters in the calorimeter with  $\geq 60\text{ MeV}$ . We also required no activity in the CV and in some other photon counters.

Analysis procedures were basically the same as described in [4]. First, we identified clusters in the calorimeter, each of which should have transverse shower shape consistent with a single photon. The clusters were required to have more than  $150$  and  $250\text{ MeV}$  for the lower and higher energy photons from  $\pi^0$ , respectively. To improve the accuracy of energy measurement, clusters within the  $36 \times 36\text{ cm}^2$  square around the beam and outside the radius of  $88\text{ cm}$  were not used as the photon candidates. Second, we selected events with exactly two photons in the calorimeter and without any in-time hits in the other counters. In order to achieve high efficiency of particle detection [7], energy thresholds for the counters were set at around  $1\text{ MeV}$ ; e.g.  $1.0\text{ MeV}$  for FB, MB, and CC02, and  $0.3\text{ MeV}$  for CV. An additional photon counter (BA) was placed in the beam at the downstream end. It consisted of a series of alternating layers of lead, quartz, and scintillator plates. Photons to the BA were identified by the Čerenkov light in the quartz

layers and by the energy deposition of more than  $20\text{ MeV}$  in the scintillator layers. Third, assuming that two photons came from a  $\pi^0$  decay on the beam axis, we calculated the decay vertex position along the beam axis ( $Z$ ) and the transverse momentum of  $\pi^0$  ( $P_T$ ). Fourth, we imposed kinematic requirements as follows. To remove  $K_L^0 \rightarrow \gamma\gamma$  decays, we calculated the opening angle between two photon directions projected on the calorimeter plane, and required it to be  $\leq 135$  degrees. The shower shape was required to be consistent with a photon entering the calorimeter with the direction from the decay vertex to the hit position on the surface. The reconstructed  $\pi^0$  should have the energy less than  $2\text{ GeV}$ , and should be kinematically consistent with a  $K_L^0 \rightarrow \pi^0\nu\bar{\nu}$  decay within the proper  $K_L^0$  momentum range. Finally, we defined the region for the candidate events (signal box) in the  $P_T$  vs  $Z$  plot as  $0.12 < P_T < 0.24\text{ GeV}/c$  and  $340 < Z < 500\text{ cm}$ . In this analysis, we masked the signal box so that all the selection criteria (cuts) were determined without examining the candidate events.

There were two types of background events. One was the events from  $K_L^0$  decays and the other was the events due to the neutrons in the halo of the neutral beam (“halo neutrons”).

The main background source from  $K_L^0$  decays was the  $K_L^0 \rightarrow \pi^0\pi^0$  mode, whose branching ratio is  $8.7 \times 10^{-4}$ . There are four photons in the final state, and if two of them escape detection,  $K_L^0 \rightarrow \pi^0\pi^0$  can fake a signal event. The number of background events was estimated by Monte Carlo simulation. We generated  $K_L^0 \rightarrow \pi^0\pi^0$  decays with 11 times larger statistics than the data. After imposing all the cuts, the background level was estimated to be  $0.11$  events. It turned out that the CsI calorimeter and the main barrel were the most responsible components for detecting extra photons and rejecting those backgrounds. To verify the detection inefficiency of photon counters in the simulation, we analyzed the events with four photons reconstructed in the calorimeter. As shown in Fig. 2, in addition to the  $K_L^0 \rightarrow \pi^0\pi^0$  events at the  $K_L^0$  mass, there was a tail in the lower mass region due to contamination from  $K_L^0 \rightarrow 3\pi^0$ , whose two out of six photons escaped detection. The number of events in the tail was reproduced by our simulation [8]. For charged decay modes ( $K_L^0 \rightarrow \pi^+\pi^-\pi^0$ ,  $K_L^0 \rightarrow \pi l\nu$  ( $l = e, \mu$ )), we studied the rejection power of the kinematic cuts to these backgrounds. Multiplying the expected inefficiency of charged particle counters to their rejection, we estimated their contribution to be negligible.

Halo neutrons induced a substantial portion of backgrounds, although the halo was suppressed by 5 orders of magnitude from the beam core. The background was categorized into three types and they were estimated separately. The first type was due to  $\pi^0$ 's produced in the interaction of halo neutrons with the upstream CC02 collar counter (“CC02 BG”). Ideally, their  $Z$  position should be reconstructed properly at CC02, *i.e.*, outside the signal

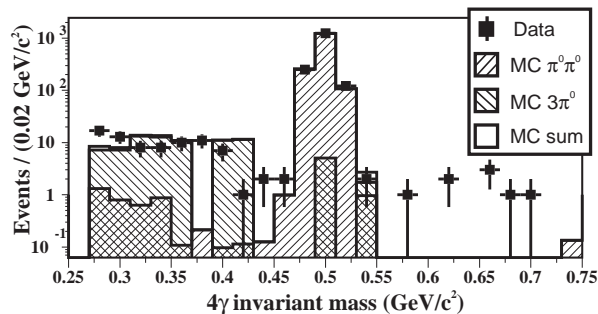


FIG. 2: Reconstructed invariant mass distribution of the events with four photons in the calorimeter. The points show the data, and the histograms indicates the contribution of  $K_L^0 \rightarrow \pi^0\pi^0$  and  $K_L^0 \rightarrow 3\pi^0$  decays (and their sum), expected from the simulation, normalized with the number of events in the  $K_L^0 \rightarrow \pi^0\pi^0$  peak.

box. However, they can enter the signal region when the energy of either photon was mismeasured due to shower leakage or photo-nuclear interactions in the calorimeter. To reproduce the tail in the vertex distribution, we used data obtained in a dedicated run for the study (“Al plate run”), in which a 0.5-cm-thick aluminum plate was inserted to the beam at 6.5 cm downstream of the rear end of CC02 [9]. After imposing analysis cuts and selecting events with two photons in the calorimeter whose invariant mass was consistent with  $\pi^0$ , we obtained the distribution of reconstructed Z vertex of  $\pi^0$ 's produced at the Al plate. It was then convoluted with the Z distribution of  $\pi^0$ 's production points within CC02 [10] so as to match the peak position with that observed in the physics run, as shown in Fig. 3. The distribution was normalized to the number of events in  $Z < 300$  cm. We estimated the number of CC02 BG events inside the signal box to be 0.16.

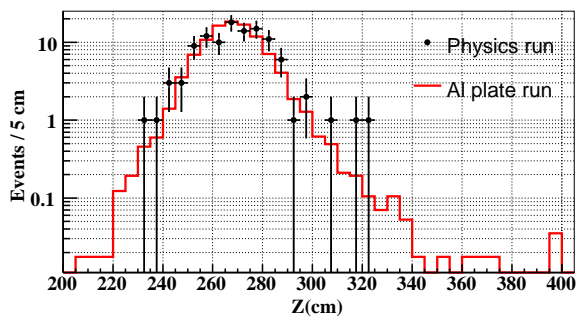


FIG. 3: (color online) Reconstructed Z vertex distribution of  $\pi^0$ 's produced within CC02. The points show the data in the physics run in the upstream region ( $Z < 340$  cm) and the histogram indicates the distribution from the Al plate run.

The second type of neutron-induced background was due to neutron interactions with the CV (“CV BG”). This background should also be reconstructed properly at the Z position of the CV, *i.e.*, outside the signal box.

However, events can shift upstream when either cluster was overlapped by other associated particles and thereby mismeasured, or when one of the clusters (or both) was in fact not due to a photon from  $\pi^0$ . In order to evaluate the background level inside the signal box, we performed a bifurcation study with data [11, 12]. In the simulation studied beforehand, the cuts against extra particles and the shower shape cut turned out to be efficient in the background reduction; these cuts were chosen as two uncorrelated cut sets in the bifurcation study. The rejection power of one cut set was evaluated with inverting another cut set, and vice versa. Multiplying the obtained rejection factors, the number of CV BG events inside the signal box was estimated to be 0.08.

The third type of neutron-induced background was due to  $\eta$ 's produced by the halo through interactions with the CV (“CV- $\eta$  BG”). Since the Z vertex position was calculated by assuming the  $\pi^0$  mass,  $\eta$ 's were reconstructed about four times farther away from the calorimeter, and they can fall into the signal box. To simulate the  $\eta$  production, we used a GEANT4-based simulation with the Binary Cascade hadron interaction model [13]. Figure 4 demonstrates the simulation, which reproduced the invariant mass distribution (from  $\pi^0$  mass to  $\eta$  mass) of the events with two photons in the calorimeter from the Al plate run, normalized by the number of protons on the target. We then simulated  $\eta$  production at the CV and estimated the number of CV- $\eta$  BG events inside the signal box to be 0.06.

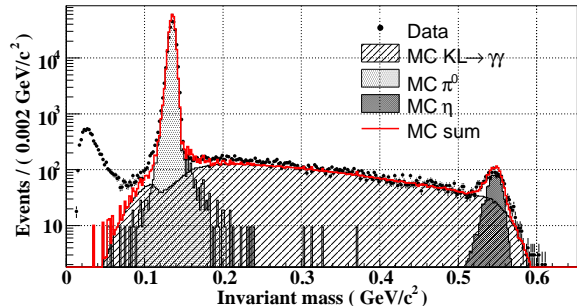


FIG. 4: (color online) Reconstructed invariant mass distribution of the two photon events in the Al plate run, explained in the text. Points with error bars show the data. Histograms indicate the contributions from  $\pi^0$  and  $\eta$  produced in the Al plate,  $K_L^0 \rightarrow \gamma\gamma$  decays, and their sum, respectively, from the simulation. Events in the low mass region were considered to be due to neutron interactions accompanying neither  $\pi^0$ 's nor  $\eta$ 's, which were not recorded in the simulation.

Table I summarizes the estimated numbers of background events inside the signal box. We also examined the numbers of events observed in several regions around the signal box, and they were statistically consistent with the estimates.

After determining all the selection criteria and estimating background levels, we examined the events in the

TABLE I: Estimated numbers of background events (BG) inside the signal box.

Background source	Estimated number of BG
$K_L^0 \rightarrow \pi^0 \pi^0$	$0.11 \pm 0.09$
CC02	$0.16 \pm 0.05$
CV	$0.08 \pm 0.04$
CV- $\eta$	$0.06 \pm 0.02$
total	$0.41 \pm 0.11$

signal box and found no candidates, as shown in Fig. 5.

The number of collected  $K_L^0$  decays was estimated using the  $K_L^0 \rightarrow \pi^0 \pi^0$  decay, based on 1495 reconstructed events, and was cross-checked by measuring  $K_L^0 \rightarrow 3\pi^0$  and  $K_L^0 \rightarrow \gamma\gamma$  decays [14]. The 5% discrepancy observed between these modes was accounted for as an additional systematic uncertainty. The single event sensitivity for the  $K_L^0 \rightarrow \pi^0 \nu \bar{\nu}$  branching ratio is given by

$$S.E.S.(K_L^0 \rightarrow \pi^0 \nu \bar{\nu}) = \frac{1}{\text{Acceptance} \cdot N(K_L^0 \text{ decays})},$$

where the acceptance includes the geometrical acceptance, the analysis efficiency, and the acceptance loss due to accidental hits. Using the total acceptance of 0.67% and the number of  $K_L^0$  decays of  $5.1 \times 10^9$ , the single event sensitivity was  $(2.9 \pm 0.3) \times 10^{-8}$ , where the error includes both statistical and systematic uncertainties.

Since we observed no events inside the signal box, we set an upper limit for the  $K_L^0 \rightarrow \pi^0 \nu \bar{\nu}$  branching ratio,

$$Br(K_L^0 \rightarrow \pi^0 \nu \bar{\nu}) < 6.7 \times 10^{-8} \text{ (90\% C.L.)},$$

based on the Poisson statistics. In deriving the limit, the uncertainty of the single event sensitivity was not taken into consideration. The result improves the previous limit [4] by a factor 3, and the background level by an order of magnitude.

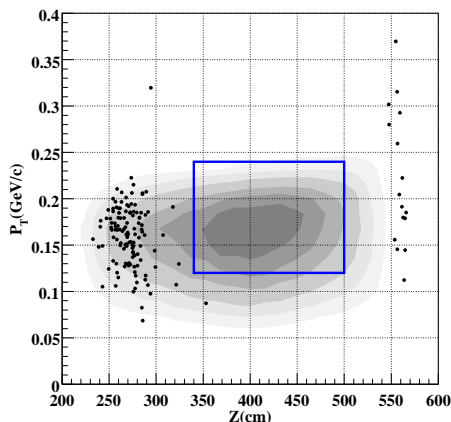


FIG. 5: (color online) Scatter plot of  $P_T$  vs reconstructed  $Z$  position after imposing all the cuts. The points show the data and the contour represents the simulated distribution of the signal. The rectangle indicates the signal region.

We are grateful to the continuous support by KEK and the successful beam operation by the crew of the KEK 12-GeV proton synchrotron. This work has been partly supported by a Grant-in-Aid from the MEXT and JSPS in Japan, a grant from NSC in Taiwan, a grant from KRF in Korea, and the U.S. Department of Energy.

\* Present address: Laboratory of Nuclear Problems, Joint Institute for Nuclear Research, Dubna, Moscow Region, 141980 Russia

† Present address: Scarina Gomel' State University, Gomel', BY-246699, Belarus

‡ Present address: Institute of Particle and Nuclear Studies, High Energy Accelerator Research Organization (KEK), Tsukuba, Ibaraki, 305-0801 Japan

§ Deceased.

¶ Present address: RIKEN SPring-8 Center, Sayo, Hyogo, 679-5148 Japan

- [1] L. S. Littenberg, Phys. Rev. D **39**, 3322 (1989).
- [2] D. Bryman *et al.*, Int. J. Mod. Phys. **21**, 487 (2006); A. J. Buras *et al.* hep-ph/0405132, and references therein.
- [3] F. Mescia and C. Smith, Phys. Rev. D **76**, 034017 (2007).
- [4] J. K. Ahn *et al.*, Phys. Rev. D **74**, 051105(R) (2006).
- [5] H. Watanabe *et al.*, Nucl. Instr. Meth. Phys. Res., Sect. A **545**, 542 (2005).
- [6] M. Doroshenko *et al.*, Nucl. Instr. Meth. Phys. Res. Sect. A **545**, 278 (2005); M. Doroshenko, Ph.D. thesis, The Graduate University for Advanced Science, 2005; K. Sakashita, Ph.D. thesis, Osaka University, 2006.
- [7] S. Ajimura *et al.*, Nucl. Instr. Meth. Phys. Res., Sect. A **435**, 408 (1999); S. Ajimura *et al.*, Nucl. Instr. Meth. Phys. Res., Sect. A **552**, 263 (2005); T. Inagaki *et al.*, Nucl. Instr. Meth. Phys. Res., Sect. A **359**, 478 (1995).
- [8] Events in the higher mass region come from  $K_L^0 \rightarrow 3\pi^0$  with mis-combination(s) of photons. The discrepancy is due to the small sample size of the simulation.
- [9] The neutron spectra in the core and halo regions of the beam were different. However, it was found that, when two photons from  $\pi^0$  were detected in the calorimeter, the energy and transverse momentum distributions of the  $\pi^0$ 's produced at the CC02 by the core neutrons were similar to those of the  $\pi^0$ 's by the halo neutrons.
- [10] We confirmed by simulation studies the  $Z$  distribution of  $\pi^0$ 's produced within CC02 was expressed as an exponential of the distance from the rear end of the CC02.
- [11] S. Adler *et al.*, Phys. Rev. Lett. **79**, 2204 (1997).
- [12] J. Nix *et al.*, Phys. Rev. D **76**, 011101 (2007).
- [13] The detector simulation in E391a is based on the GEANT 3.21. In order to simulate the  $\eta$  production in the detector, we used the GEANT 4.8.3 with the QBBC physics list. See "GEANT3.21, CERN Program Library Long Writeup W5013"; S. Agostinelli *et al.*, Nucl. Instr. Meth. Phys. Res., Sect. A **506** 250 (2003); "Geant4 8.3 Release Notes", CERN.
- [14] The branching ratio of each  $K_L^0$  decay mode was taken from W.-M. Yao *et al.* (Particle Data Group), J. Phys. G **33**, 1 (2006) ; <http://pdg.lbl.gov/> .